Photonic Band Gap Architectures for Holographic Lithography

Ovidiu Toader, Timothy Y. M. Chan, and Sajeev John

Department of Physics, University of Toronto, 60 St. George Street, Toronto, Ontario, Canada M5S 1A7

(Received 5 August 2003; published 30 January 2004)

Using symmetry considerations, we identify three families of large photonic band-gap (PBG) architectures defined by the isointensity surfaces of four beam laser interference. For particular choices of beam intensities, directions, and polarizations, we obtain a diamondlike crystal, a novel body-centered cubic architecture, and a simple cubic structure with PBG to center frequency ratios of 25%, 21%, and 11%, respectively, when the isointensity surface defines a silicon (dielectric constant of 11.9) to air boundary.

DOI: 10.1103/PhysRevLett.92.043905 PACS numbers: 42.70.Qs

Photonic band-gap (PBG) materials [1,2] are periodically ordered dielectric microstructures that facilitate the localization of light [3,4]. This provides a fundamental platform for the integration of active and passive devices into an all-optical microchip [5]. The efficient microfabrication of high quality PBG materials has been a major scientific challenge over the past decade. While considerable attention has focused on layer-by-layer microlithography [6,7] and self-assembly techniques [8,9], the achievement of long range order (LRO) on the scale of hundreds of lattice constants has been difficult. In the holographic lithography (HL) method, recently introduced by Campbell *et al.* [10], nearly perfect LRO can be maintained over arbitrary length scales using the three-dimensional (3D) interference pattern of four laser beams in a photoresist material [11–14]. When the total light intensity, $I(\vec{\mathbf{r}})$, at position $\vec{\mathbf{r}}$, is maintained over a time interval $\delta\tau$ such that the "exposure" $I(\vec{\mathbf{r}})\delta\tau$ exceeds a specified threshold, T, the photoresist in the vicinity of $\vec{\mathbf{r}}$ is chemically altered. This "overexposed" region can be selectively removed using a developer substance which leaves the "underexposed" regions intact. The developed photoresist then acts as a 3D photonic crystal (PC) template which is infiltrated with SiO_2 [15]. The photoresist is then burned away, leaving behind a daughter "inverse" template. Finally, the daughter template is inverted by infiltration with silicon [8,9] and selective chemical etching of the SiO_2. The result is a 3D silicon PC, in which the silicon-air boundary is defined by the isointensity surface $I(\vec{\mathbf{r}})\delta\tau = T$. Despite the enormous potential offered by HL for efficient and accurate synthesis of 3D PCs, a major unsolved theoretical problem is the identification of holographic beam intensities, polarizations, and directions that lead to a large and complete 3D PBG.

In this Letter, we present a detailed theoretical road map for achieving large 3D photonic band gaps using holographic lithography. Previously published theoretical reports have either focused on only a partial set of parameters [16,17] or considered [18–20] the isosurface separating the underexposed and overexposed phases as a particular case of triply periodic minimal surfaces [21]. In contrast, we present physical, intuitive results based on point group and space group symmetries. We demonstrate that holographic beam parameters can be chosen to recapture essential features of the diamond lattice structure, leading to an architecture with a complete PBG (after replication with Si, $\varepsilon = 11.9$) of more than 25%. We also introduce a new family of body-centered cubic (bcc) architectures. Remarkably, the optimized bcc crystal exhibits a PBG (after replication with Si) of 21%. This serves as a striking alternative to the prevailing view that only face-centered cubic (fcc) PCs are suitable for observing a large 3D PBG.

The interference of N monochromatic plane waves of frequency ω, propagation vectors $\vec{G}_i$, linear polarization vectors $\vec{\boldsymbol{\epsilon}}$, phases ϕ_i, and real amplitudes $\mathcal{E}_i$ creates a field given by $\vec{E}(\vec{\mathbf{r}}, t) = e^{-i\omega t} e^{i(\vec{G}_0\cdot\vec{\mathbf{r}}+\phi_0)}(\mathcal{E}_0\vec{\boldsymbol{\epsilon}}_0 + \sum_{i=1}^{N-1} \times \mathcal{E}_i\vec{\boldsymbol{\epsilon}}_i\, e^{i(\vec{K}_i\cdot\vec{\mathbf{r}}+\gamma_i)})$, where $\vec{K}_i \equiv \vec{G}_i - \vec{G}_0$ and $\gamma_i \equiv \phi_i - \phi_0$. The corresponding, stationary intensity pattern is given by

$$I(\vec{\mathbf{r}}) \equiv \vec{E}^*(\vec{\mathbf{r}}, t)\cdot\vec{E}(\vec{\mathbf{r}}, t) = \sum_{i=0}^{N-1}\mathcal{E}_i^2 + 2\sum_{i=1}^{N-1}\mathcal{E}_0\mathcal{E}_i\,\vec{\boldsymbol{\epsilon}}_0\cdot\vec{\boldsymbol{\epsilon}}_i\cos(\vec{K}_i\cdot\vec{\mathbf{r}} + \gamma_i) + 2\sum_{i>j=1}^{N-1}\mathcal{E}_i\mathcal{E}_j\,\vec{\boldsymbol{\epsilon}}_i\cdot\vec{\boldsymbol{\epsilon}}_j\cos[(\vec{K}_i - \vec{K}_j)\cdot\vec{\mathbf{r}} + \gamma_i - \gamma_j]. \tag{1}$$

In the following, we consider only the case $N = 4$ which provides the minimum number of beams required to produce a nontrivial 3D intensity pattern. The holographic structure is a two components medium defined by the "shape" function $\Theta[I(\vec{\mathbf{r}}) - I_{\text{thr}}^{\text{exp}}]$, where $I_{\text{thr}}^{\text{exp}}$ is a threshold value and $\Theta = 1$ for $x \geq 0$ and zero otherwise (Heaviside step function). By convention, we assume the high intensity regions in Eq. (1) become the silicon component of the photonic crystal [$\boldsymbol{\varepsilon}(\vec{\mathbf{r}}) = 1$ where $I(\vec{\mathbf{r}}) < I_{\text{thr}}^{\text{exp}}$ and $\boldsymbol{\varepsilon}(\vec{\mathbf{r}}) = 11.9$ where $I(\vec{\mathbf{r}}) \geq I_{\text{thr}}^{\text{exp}}$].

 0031-9007/04/92(4)/043905(4)$22.50

For a given $\vec{G}_i$, it is convenient to introduce the orthonormal triad of vectors $\vec{R}_i = \vec{G}_i \times \hat{\mathbf{z}}/|\vec{G}_i \times \hat{\mathbf{z}}|$, $\vec{U}_i = \vec{R}_i \times \vec{G}_i/|\vec{G}_i|$, and $\vec{U}_i \times \vec{R}_i = \vec{G}_i/|\vec{G}_i|$, where $(\hat{\mathbf{x}}, \hat{\mathbf{y}}, \hat{\mathbf{z}})$ define unit vectors in a specific laboratory coordinate frame. (If $\vec{G}_i || \hat{\mathbf{z}}$, then by convention we choose $\vec{R}_i = \hat{\mathbf{x}}$.)

The polarization vector can be expressed in terms of $\vec{U}_i$, $\vec{R}_i$, and a polarization angle, φ_i, as $\vec{\epsilon}_i = \cos(\varphi_i)\vec{U}_i + \sin(\varphi_i)\vec{R}_i$. In the case of the four beam configuration, Eq. (1) becomes $I(\vec{\mathbf{r}}) = I_0 + 2\Delta I(\vec{\mathbf{r}})$ where $I_0 \equiv \mathcal{E}_0^2 + \mathcal{E}_1^2 + \mathcal{E}_2^2 + \mathcal{E}_3^2$ and

$$\Delta I(\vec{\mathbf{r}}) \equiv c_1 \cos(\vec{K}_1 \cdot \vec{\mathbf{r}} + \gamma_1) + c_2 \cos(\vec{K}_2 \cdot \vec{\mathbf{r}} + \gamma_2) + c_3 \cos(\vec{K}_3 \cdot \vec{\mathbf{r}} + \gamma_3) + c_{12} \cos(\vec{K}_{12} \cdot \vec{\mathbf{r}} + \gamma_1 - \gamma_2) + c_{13} \cos(\vec{K}_{13} \cdot \vec{\mathbf{r}} + \gamma_1 - \gamma_3) + c_{23} \cos(\vec{K}_{23} \cdot \vec{\mathbf{r}} + \gamma_2 - \gamma_3), \quad (2)$$

where

$$c_i = \mathcal{E}_0 \mathcal{E}_i \vec{\epsilon}_0 \cdot \vec{\epsilon}_i; \qquad c_{ij} = \mathcal{E}_i \mathcal{E}_j \vec{\epsilon}_i \cdot \vec{\epsilon}_j; \quad (3)$$

$$\vec{K}_{ij} = \vec{K}_i - \vec{K}_j; \qquad \vec{K}_i = \vec{G}_i - \vec{G}_0. \quad (4)$$

The phase factors in Eq. (2) are irrelevant because they can be simultaneously eliminated [22]. By rewriting the "experimental" intensity threshold as $I_{\text{thr}}^{\text{exp}} = I_0 + 2I_{\text{thr}}$, we arrive at the following simplified shape function:

$$\Theta(I(\vec{\mathbf{r}}) - I_{\text{thr}}^{\text{exp}}) = \Theta(\Delta I(\vec{\mathbf{r}}) - I_{\text{thr}}). \quad (5)$$

The spatial modulation of the intensity pattern given by Eq. (2) is periodic with a lattice whose primitive vectors, $\vec{\mathbf{a}}_i$, satisfy $\vec{K}_i \cdot \vec{\mathbf{a}}_j = 2\pi\delta_{ij}$. As a consequence, the lattice constants are inversely proportional to the frequency of the laser beams.

The design problem consists of identifying the set $C = \{c_i, c_{ij}\}_{i<j=\overline{1,3}}$ of six polarization and amplitude coefficients (some possibly 0), three $\vec{K}_i$ vectors, and suitable threshold I_{thr}, which generates a photonic crystal [through the shape function given by (5)] with a complete PBG. Once C and $\vec{K}_i$ are found, the directions, amplitudes, and polarizations of the four laser beams are determined by a two-step algorithm: (1) find the four beam directions, $\{\vec{G}\}_{i=\overline{0,3}}$, which satisfy Eq. (4), (2) use $\vec{G}_i$ from stage (1) to find the four amplitudes and polarization angles, $\{\mathcal{E}_i, \phi_i\}_{i=\overline{0,3}}$, by solving the nonlinear system of six equations given by Eq. (3).

The identification of C and the choice of $\vec{K}_i$ are obtained by two guiding principles: (i) choose a given Bravais lattice, and (ii) identify architectures leading to the smallest possible irreducible Brillouin zones (IBZ). If we denote by $\{\vec{\mathbf{a}}_i, \vec{\mathbf{b}}_i\}_{i=\overline{1,3}}$ the primitive and reciprocal vectors, respectively, of the desired Bravais lattice, then criterion (i) above is automatically satisfied if $\vec{K}_i$ is a linear combination with *integral* coefficients of vectors from the set $\{\vec{\mathbf{b}}\}$. Condition (ii), however, is far more restrictive. Indeed, only a very limited set of C, $\vec{K}_i$ combinations generate an intensity pattern with a sufficiently high symmetry. Suppose that the desired holographic structure has a cubic symmetry [simple cubic (sc), bcc, or fcc]. Sorted by their lengths, the first three sets of vectors in the cubic reciprocal space are $\mathcal{B}^s = \{\pm\vec{\mathbf{b}}_i^s\}$ of length $2\pi/\mathbf{a}$, $\mathcal{B}^b = \{\pm\vec{\mathbf{b}}_i^b\} \bigcup \{\vec{\mathbf{b}}_i^b - \vec{\mathbf{b}}_j^b\}_{i\neq j}$ of length $2\pi\sqrt{2}/\mathbf{a}$, and $\mathcal{B}^f = \{\pm\vec{\mathbf{b}}_i^f\} \bigcup \{\pm(\vec{\mathbf{b}}_1^f + \vec{\mathbf{b}}_2^f + \vec{\mathbf{b}}_3^f)\}$ of length $2\pi\sqrt{3}/\mathbf{a}$. i and j run from 1 to 3, and $\vec{\mathbf{b}}_i^*$ denote the three primitive vectors of the sc (**s**), bcc (**b**), and fcc (**f**) reciprocal lattices, respectively. We define the set $\mathcal{T}$ of "target vectors" as a subset $\mathcal{T} \subset \mathcal{K} \equiv \{\vec{K}_1, \vec{K}_2, \vec{K}_3, \vec{K}_{12}, \vec{K}_{13}, \vec{K}_{23}\}$ corresponding to nonzero terms in Eq. (2) (or, equivalently, nonzero coefficients in C). Accordingly, we define $C_{\mathcal{T}} \subset C$ as the subset of nonzero coefficients of C. Clearly, the requirement of high symmetry can be achieved by choosing $\mathcal{T}$ simply to be a subset of one of the reciprocal lattice basis vector sets $\mathcal{B}^*$. Since $\Delta I(\vec{\mathbf{r}})$ is insensitive to the sign of the target vectors in $\mathcal{T}$, an upper bound on the size of the sets $\mathcal{T}$ and $C_{\mathcal{T}}$ is 3 in the case of $\mathcal{B}^s$, 6 in the case of $\mathcal{B}^b$, and 4 in the case of $\mathcal{B}^f$.

We first illustrate the choice of C coefficients using the fcc Bravais lattice. Since there are only four distinct directions in the $\mathcal{B}^f$ set, the target vector set can be denoted as $\mathcal{T} = \{\vec{T}_1, \vec{T}_2, \vec{T}_3, \vec{T}_4\}$. One possible choice for the three $\vec{K}_i$ vectors is $\vec{K}_1 = \frac{2\pi}{\mathbf{a}}(1, 1, 1)$, $\vec{K}_2 = \frac{2\pi}{\mathbf{a}}(0, 2, 0)$, and $\vec{K}_3 = \frac{2\pi}{\mathbf{a}}(-1, 1, 1)$. This leads to the choice $\mathcal{T} = \{\vec{K}_3, \vec{K}_{12}, \vec{K}_{23}, \vec{K}_1\}$, and $C = \{*, 0, *, *, 0, *\}$ where $*$ indicates a nonzero real coefficient. We denote the nonzero target coefficients as $C_{\mathcal{T}} = \{\tau_1, \tau_2, \tau_3, \tau_4\}$ and Eq. (2) becomes $\Delta I(\vec{\mathbf{r}}) = \sum_{i=1}^4 \tau_i \cos(\vec{T}_i \cdot \vec{\mathbf{r}})$. We define $\mathcal{O}^d = \{\mathcal{O}_j^d\}_{j=\overline{1,48}}$ as the set of fcc point group operations. The requirement for the smallest possible IBZ corresponds to choosing $C_{\mathcal{T}}$ and finding a translation vector, $\vec{\delta}$, such that $\Delta I(\vec{\mathbf{r}})$ is invariant under changes of the form $\vec{\mathbf{r}} \to S_{\mathbf{j},\vec{\delta}}^d(\vec{\mathbf{r}}) \equiv \mathcal{O}_{\mathbf{j}}^{\mathbf{d}}(\vec{\mathbf{r}}) + \vec{\delta}$:

$$\Delta I(\vec{\mathbf{r}}) \xrightarrow{S_{\mathbf{j},\vec{\delta}}^d} \sum_{i=1}^4 \tau_i \cos(\vec{T}_i \cdot S_{\mathbf{j},\vec{\delta}}^d(\vec{\mathbf{r}})) = \sum_{i=1}^4 \tau_i \cos[\mathcal{O}_j^r(\vec{T}_i) \cdot \vec{\mathbf{r}} + \xi_i]. \quad (6)$$

Here, $\mathcal{O}^r = \{\mathcal{O}_j^r\}_{j=\overline{1,48}}$ is the set of point group operations of the fcc reciprocal space, and $\{\xi_i = \vec{T}_i \cdot \vec{\delta}\}_{i=\overline{1,4}}$ is a set of four phase factors. ξ_i are not independent because they are related to $\gamma_i = \vec{K}_i \cdot \vec{\delta}$. For our particular choice of target vectors, it can be verified that $\mathcal{O}_j^r(\vec{T}_i) \in \{\pm\vec{T}_1, \pm\vec{T}_2, \pm\vec{T}_3, \pm\vec{T}_4\}$. Since the sign of $\vec{T}_i$ leaves $\Delta I(\vec{\mathbf{r}})$ unchanged, it follows that the point group operations $\mathcal{O}_j^d$ simply permute the coefficients $\{\tau_i\}$ as they appear in (6). Invariance of $\Delta I(\vec{\mathbf{r}})$ can, therefore, be enforced by requiring $|\tau_i| = 1$ for each i and using $\vec{\delta}$ to compensate for any sign changes (induced by permutation) in (6). Accordingly, we assume that $\gamma_i, \xi_i \in \{0, \pi\}$. The eight possible phase configurations are described by the sign vectors defined as $\Sigma^k \equiv \{e^{i\gamma_1}, e^{i\gamma_2}, e^{i\gamma_3}, e^{i(\gamma_1-\gamma_2)}, e^{i(\gamma_1-\gamma_3)}, e^{i(\gamma_2-\gamma_3)}\}$, where $k = \overline{1,8}$

corresponds to one of the 2^3 possible choices for the $\{\gamma_1, \gamma_2, \gamma_3\}$ set. It follows that

$$\Delta I(\vec{\mathbf{r}}) = \sum_{i=1}^{4} \tau_i \cos(\vec{T}_i \cdot \vec{\mathbf{r}}) \overset{S_{j,\delta}^{d}}{\rightarrow} \sum_{i=1}^{4} \Sigma_i^k \tau_{\tau_{\mathcal{P}_j}(i)} \cos(\vec{T}_i \cdot \vec{\mathbf{r}}),$$

where $\mathcal{P}_j$ is a permutation of the indices $\{1, 2, 3, 4\}$ completely determined by $\mathcal{O}_j^d$ and Σ^k is one of the eight sign vectors described above.

Without loss of generality we can always choose the first three coefficients to be $+1$. This leaves us with two options for $\Delta I_{\mathrm{fcc}}(\vec{\mathbf{r}})$:

$$\Delta I_{\mathrm{fcc}}(\vec{\mathbf{r}}) = \cos(\vec{\mathbf{b}}_1^f \cdot \vec{\mathbf{r}}) + \cos(\vec{\mathbf{b}}_2^f \cdot \vec{\mathbf{r}}) + \cos(\vec{\mathbf{b}}_3^f \cdot \vec{\mathbf{r}}) + \eta \cos[(\vec{\mathbf{b}}_1^f + \vec{\mathbf{b}}_2^f + \vec{\mathbf{b}}_3^f) \cdot \vec{\mathbf{r}}], \quad (7)$$

where $\eta = \pm 1$ and $\{\vec{\mathbf{b}}_i^F\}$ are the primitive vectors of the fcc reciprocal space. The choice $\eta = +1$ leads to an intensity pattern which resembles the opal structure [see Fig. 1(a)]. However, when $\eta = -1$ the intensity pattern exhibits a strong resemblance to a diamond network structure [see Fig. 1(b)]. The single sign which differentiates the fcc-opal versus diamond structures in Eq. (7) is crucial to the photonic band structure. Whereas in the case $\eta = +1$ the fundamental band gap does not open, in the case $\eta = -1$ a gap as large as 25% opens between second and third bands in a structure whose solid component has a dielectric constant of 11.9 (Si). In the HL technique, this sign can be controlled directly through the amplitude and polarization of the laser beams. The beam parameters in the $\eta = -1$ case are the following: (i) wave vectors $\vec{G}_0 = \frac{\pi}{\mathbf{a}}(0, -2, -1)$, $\vec{G}_1 = \frac{\pi}{\mathbf{a}}(2, 0, 1)$, $\vec{G}_2 = \frac{\pi}{\mathbf{a}}(0, 2, -1)$, and $\vec{G}_3 = \frac{\pi}{\mathbf{a}}(-2, 0, 1)$, (ii) amplitudes $\{\mathcal{E}_0, \mathcal{E}_1, \mathcal{E}_2, \mathcal{E}_3\} = \{A, B, B, B\}$ where $A/B = 1/\sqrt{17}$, and (iii) polarizations $\{\varphi_0, \varphi_1, \varphi_2, \varphi_3\} = \{350.4°, 244.3°, 105.7°, 16.1°\}$.

The procedure described above can be applied to any Bravais lattice. A particularly interesting case is the bcc lattice, which has remained largely unexplored in the photonic crystal literature. In this case, the target vectors are chosen from the set $\mathcal{B}^b$. To create an intensity pattern whose IBZ is as small as that of the bcc Bravais lattice, all six target vectors (the sign of the vectors is irrelevant) are needed. Unfortunately, the resulting structure is too symmetric and the fundamental PBG does not open. Therefore, we consider a subset of four out of the six available directions. This leads to a larger IBZ and an intensity pattern of lower symmetry. Figure 2 displays the holographic isointensity surface for the optimized bcc architecture:

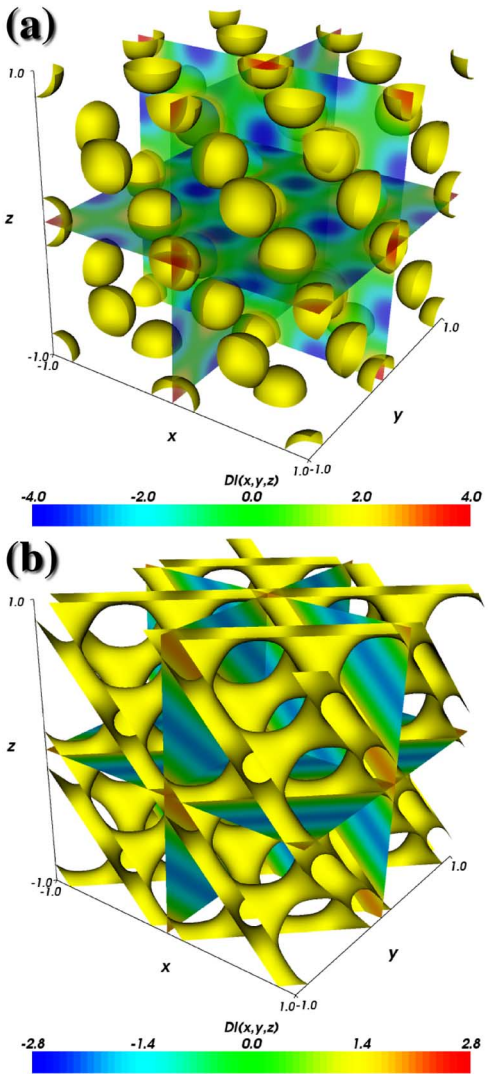

FIG. 1 (color online). The isointensity surfaces of the fcc structure generated by Eq. (7). (a) An opal-like architecture appears for $\eta = +1$. (b) A diamondlike architecture appears for $\eta = -1$. In both cases, the light intensity is mapped to the color bar.

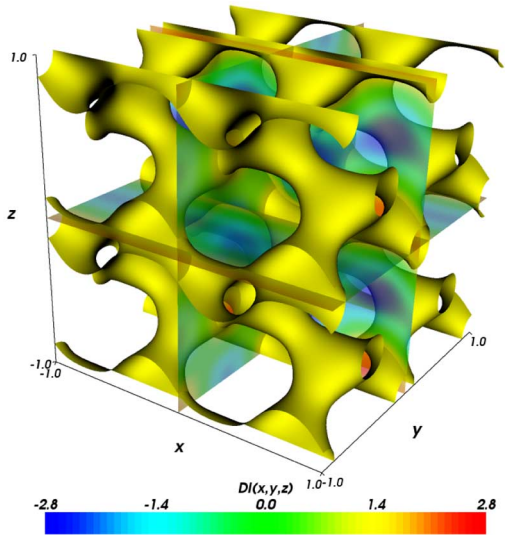

FIG. 2 (color online). The optimized bcc architecture generated by Eq. (8) with a solid volume filling fraction of $\approx 22\%$. When the solid regions (interior of depicted isointensity surfaces) consist of silicon and the background is air, a PBG of 21% is obtained.

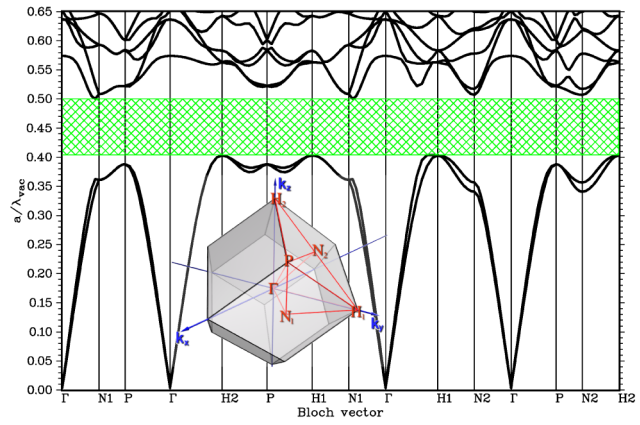

FIG. 3 (color online). The photonic band structure diagram of the optimized bcc architecture. A gap of 21%, centered at $\mathbf{a}/\lambda_{\mathrm{vac}} = 0.45$, opens between bands 2 and 3. The positions of the high symmetry points together with the IBZ are shown in the inset.

$$\Delta I_{\mathrm{bcc}}(\vec{\mathbf{r}}) = \cos(\vec{T}_1 \cdot \vec{\mathbf{r}}) + \cos(\vec{T}_2 \cdot \vec{\mathbf{r}}) + \cos(\vec{T}_3 \cdot \vec{\mathbf{r}}) - \cos(\vec{T}_4 \cdot \vec{\mathbf{r}}). \quad (8)$$

The target vectors expressed in terms of the bcc reciprocal primitive vectors are $\{\vec{T}_1, \vec{T}_2, \vec{T}_3, \vec{T}_4\} = \{\vec{\mathbf{b}}_2^b, \vec{\mathbf{b}}_1^b - \vec{\mathbf{b}}_3^b, -\vec{\mathbf{b}}_2^b + \vec{\mathbf{b}}_3^b, \vec{\mathbf{b}}_1^b\}$. For a Si volume fraction of $\approx 22\%$ this structure has a complete PBG of $\approx 21\%$ (see Fig. 3). The beam parameters in this case are the following: (i) wave vectors $\vec{G}_0 = \frac{\pi}{\mathbf{a}}(-1,-1,-1)$, $\vec{G}_1 = \frac{\pi}{\mathbf{a}}(-1,1,1)$, $\vec{G}_2 = \frac{\pi}{\mathbf{a}}(1,1,-1)$, and $\vec{G}_3 = \frac{\pi}{\mathbf{a}}(1,-1,1)$, (ii) amplitudes $\{\mathcal{E}_0, \mathcal{E}_1, \mathcal{E}_2, \mathcal{E}_3\} = \{A, A, B, B\}$ where $\{A, B\} = \{1.970, 1.098\}$, and (iii) polarizations $\{\varphi_0, \varphi_1, \varphi_2, \varphi_3\} = \{72.2°, 338.4°, 6.1°, 319.9°\}$.

We have also found a simple cubic holographic architecture, $\Delta I_{\mathrm{sc}}(\vec{\mathbf{r}}) = \sum_{i=1}^{3} \cos(\vec{\mathbf{b}}_i^s \cdot \vec{\mathbf{r}})$, exhibiting a PBG of roughly 11% in the case of Si:air materials. Further details of this and other structures will be presented elsewhere [23]. Figure 4 displays the variation of the relative size of the PBG with the Si volume fraction for the three holographic structures described above.

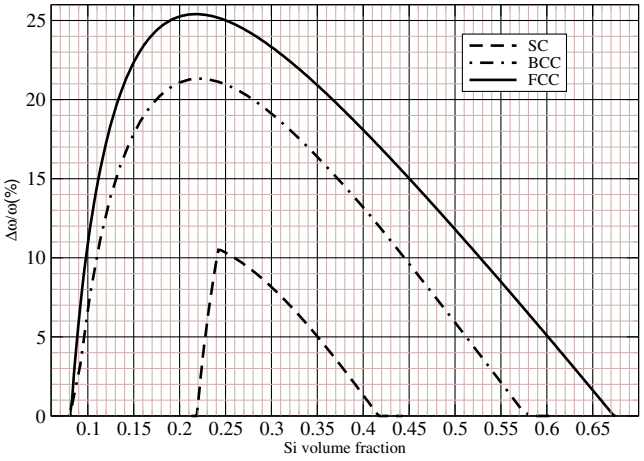

FIG. 4 (color online). Relative size of the full PBG of the sc, bcc, and fcc architectures as a function of the solid volume fraction. The solid has a dielectric constant of 11.9.

In summary, we have introduced a road map for the use of holographic lithography to create sc, fcc, and bcc photonic crystals with large 3D photonic band gaps. Our results reveal that an optimized geometrical structure within the unit cell enables the bcc lattice to exhibit a PBG comparable to that of widely studied diamond lattices. Provided that the local geometry consists of four "ligands" of suitable shape emanating from a set of nodes to form a connected network of "bonds," a PBG of more than 20% is found in both fcc and bcc lattices. This revives a fundamental question, whether long range periodicity is, in fact, essential for PBG formation or whether appropriate forms of short range order in a disordered network may suffice.

[1] Sajeev John, Phys. Rev. Lett. **58**, 2486 (1987).
[2] Eli Yablonovitch, Phys. Rev. Lett. **58**, 2059 (1987).
[3] Sajeev John, Phys. Rev. Lett. **53**, 2169 (1984).
[4] S. John and J. Wang, Phys. Rev. Lett. **64**, 2418 (1990).
[5] Alongkarn Chutinan, Sajeev John, and Ovidiu Toader, Phys. Rev. Lett. **90**, 123901 (2003).
[6] S. Y. Linetal., Nature (London) **394**, 251 (1998).
[7] S. Noda, K. Tomoda, N. Yamamoto, and A. Chutinan, Science **289**, 604 (2000).
[8] A. Blanco *et al.*, Nature (London) **405**, 437 (2000).
[9] Y. A.Vlasov, X.-Z. Bo, J. C. Sturm, and D. J. Norris, Nature (London) **414**, 289 (2001).
[10] M. Campbell *et al.*, Nature (London) **404**, 53 (2000).
[11] S. Shoji and S. Kawata, Appl. Phys. Lett. **76**, 2668 (2000).
[12] Yu. V. Miklyaev *et al.*, Appl. Phys. Lett. **82**, 1284 (2003).
[13] I. Divliansky, T. S. Mayer, K. S. Holliday, and V. H. Crespi, Appl. Phys. Lett. **82**, 1667 (2003).
[14] X. Wang *et al.*, Appl. Phys. Lett. **82**, 2212 (2003).
[15] H. Míguez *et al.*, Chem. Commun. **2002**, 2736 (2002).
[16] K. I. Petsas, A. B. Coates, and G. Grynberg, Phys. Rev. A **50**, 5173 (1994).
[17] L. Z. Cai, X. L. Yang, and Y. R. Wang, J. Opt. Soc. Am. A **19**, 2238 (2002).
[18] L. Martín-Moreno, F. J. García-Vidal, and A. M. Somoza, Phys. Rev. Lett. **83**, 73 (1999).
[19] V. Babin, P. Garstecki, and R. Holyst, Phys. Rev. B **66**, 235120 (2002).
[20] M. Maldovan *et al.*, Phys. Rev. B **65**, 165123 (2002).
[21] M. Wohlgemuth, N. Yufa, J. Hoffman, and E. L. Thomas, Macromolecules **34**, 6083 (2001).
[22] A translation of the origin by $\vec{\boldsymbol{\rho}} = \gamma_1\vec{\boldsymbol{\eta}}_1 + \gamma_2\vec{\boldsymbol{\eta}}_2 + \gamma_3\vec{\boldsymbol{\eta}}_3$, where $\vec{\boldsymbol{\eta}}_i$ satisfy $\vec{K}_i \cdot \vec{\boldsymbol{\eta}}_j = \delta_{ij}$, eliminates all phase factors, γ_i, from the expression of $\Delta I(\vec{\mathbf{r}})$ in Eq. (2). In the case of configurations with more than four beams the phase factors cannot be simultaneously eliminated.
[23] T. Y. M. Chan, O. Toader, and S. John (to be published).